Multiple Linear Detector Off-Line Calibration

SashaGasquet[1,2], Laurent Desbat[1], and Pierre-Yves Solane[2]

[1]Univ. Grenoble Alpes, CNRS, UMR 5525, VetAgro Sup, Grenoble INP, TIMC, 38000 Grenoble, France
[2]TIAMA, 215 chemin du Grand Revoyet, F-69230 Saint-Genis-Laval, France

ABSTRACT

Imaging systems require to be calibrated. The geometric calibration consists in estimating several parameters describing the projection geometry. Just like in computer vision for cameras, intrinsic parameters characterize the internal parameters of x-ray projection system. The extrinsic parameters define the orientation and position of the acquisition system. In x-ray computed tomography (CT), the acquisition systems are generally composed of a detector and a x-ray source. The object to be reconstructed lies in-between. A perfect knowledge of the calibration parameters is needed for the reconstruction algorithm to reduce artefacts. In this paper, we focus on off-line calibration methods for 1D linear x-ray detector systems. We first introduce a calibration method for systems composed of a single linear detector. This method solves the problem of calibration in two steps using calibration objects based on four co-planar lines. Moreover, we generalize the single linear detector geometric calibration method to a multi-linear detector system. We compare four different numerical models and methods. Three are based on non-linear equation systems. Finally, we propose an adaptative calibration object.

Keywords: calibration, linear detector, multi-linear detectors, computed tomography

1. INTRODUCTION

A high accuracy geometric calibration of the acquisition system is required to perform the 3D reconstruction of an object from its projections. The algorithms rely on the perfect knowledge of the intrinsic and extrinsic parameters of the system. In x-ray cone-beam CT (CBCT), these parameters describe the relation between a 3D point and its projection point on the detector image plane. Therefore, inaccurate estimations will lead to a poor reconstruction.

Off-line calibration methods of systems using 2D detector are well-known in the computer vision literature.[1] Many methods are based on the data acquired using a perfectly known geometrical object called the calibration object. In computer vision, a well-known calibration object is the Tsai grid.[2] In x-ray CBCT, calibration methods are adapted from computer vision. Calibration objects, well suited to the circular CB geometry, composed of several balls of high density material, have been designed. The projections of the balls form an ellipse from which the calibration parameters can be estimated.[3–5]

Many computer vision methods are based on a pinhole camera model. The model relates a 3D point (X, Y, Z) lying in the scene to a 2D point (u, v) on the detector. The intrinsic parameters $\alpha_u = k_u f$, $\alpha_v = k_v f$, u_0 and v_0 are contained in the calibration matrix $\mathbf{K}_{2D} \in \mathbb{R}^{3\times4}$ where f is the focal distance, k_u and k_v are the densities of pixels along the image axes $\mathbf{u}$ and $\mathbf{v}$, respectively, and (u_0, v_0) is the principal point on the detector in the image coordinates.

$$\mathbf{K}_{2D} = \begin{bmatrix} \alpha_u & 0 & u_0 & 0 \\ 0 & \alpha_v & v_0 & 0 \\ 0 & 0 & 1 & 0 \end{bmatrix} \tag{1}$$

We define the rotation matrix $\mathbf{R} \in \mathbb{R}^{3\times3}$ and the translation vector $\mathbf{t} \in \mathbb{R}^{3\times1}$ representing the orientation and position of the camera. Therefore, the pinhole camera model is defined in the Eq. (2). The parameter s is a

Contact : s.gasquet@tiama.com

7th International Conference on Image Formation in X-Ray Computed Tomography,
edited by Joseph Webster Stayman, Proc. of SPIE Vol. 12304, 1230431
 · 0277-786X · doi: 10.1117/12.2646441

scale factor.

$$\begin{bmatrix} su \\ sv \\ s \end{bmatrix} = \mathbf{K}_{2D} \begin{bmatrix} \mathbf{R} & \mathbf{t} \\ \mathbf{0}^T & 1 \end{bmatrix} \begin{bmatrix} X \\ Y \\ Z \\ 1 \end{bmatrix} \tag{2}$$

Geometric calibration is the identification of $\mathbf{K}_{2D}$, $\mathbf{R}$ and $\mathbf{t}$. In computer vision, $\mathbf{K}_{2D}$, $\mathbf{R}$ and $\mathbf{t}$ are often estimated from sufficient projections (u, v) of 3D world points (X, Y, Z) using (2). However, these model and methods must be adapted to calibrate a linear detector. A calibration object composed of lines is more suitable to linear cameras or detectors.[6] Horaud *et al.* proposed a two-step calibration method based on four co-planar lines calibration objects. The adaptation of this method to a x-ray system with a linear detector is straight forward as both systems can be described with the same geometric pinhole model.
In this paper, we adapt and generalize the Horaud *et al.* computer vision calibration method for linear camera to a multiple linear detector x-ray system. We propose a calibration object with a minimal number of opaque lines. A total of four different methods are proposed. In addition, we present a calibration object which can be adapted to different configurations of detectors. Finally, we show the performances of the proposed methods and calibration object in numerical simulations.

2. THEORY

2.1 Geometry

The system is composed of n_{D} linear detectors, denoted D_l, $l = 1, \ldots, n_{\mathrm{D}}$, and an unique x-ray source denoted S. We denote $(\mathbf{O}, \mathbf{x}, \mathbf{y}, \mathbf{z})$ the world coordinate system centred at the origin $\mathbf{O}$. An illustration of such a system is given in the Fig. 1. Furthermore, we introduce the detector coordinate system associated to the l^{th} detector $(\mathbf{O}_l, \mathbf{u}_l, \mathbf{v}_l, \mathbf{w}_l)$ where $\mathbf{v}_l$ is the image axis, $\mathbf{w}_l$ is the axis perpendicular to $\mathbf{v}_l$ pointing towards the source and $\mathbf{u}_l = \mathbf{v}_l \times \mathbf{w}_l$. The origin of the system is the point $\mathbf{O}_l$ which is the orthogonal projection of the source S on the detector D_l. The real v_l is the coordinate of $\mathbf{O}_l$ along the linear detector, along $\mathbf{v}_l$, relative to the pixel 0 of D_l.

2.2 Single detector calibration

We start by introducing the single linear detector system calibration method derived from Horaud *et al.*[6]

Pinhole linear camera model Let's consider a point (X, Y, Z) expressed in the world coordinates system and its projection v on the linear detector D. To be seen, the point has to belong to the viewing plane Π which is defined in the Eq. (3) using three real parameters p, q and r.

$$X = pY + qZ + r \tag{3}$$

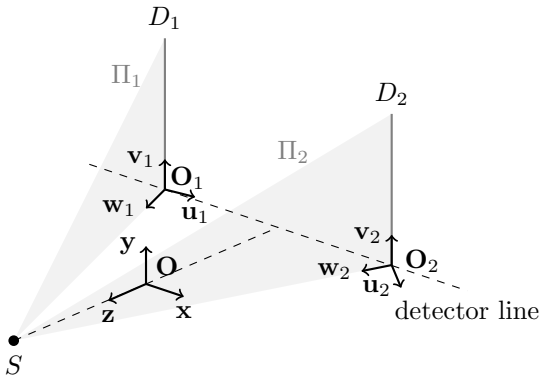

Figure 1: A two linear detector system.

Moreover, we adjust the pinhole camera model presented in the Eq. (2) to the system using a 1D detector. The rotation matrix $\mathbf{R} \in \mathbb{R}^{3\times3}$ and the translation vector $\mathbf{t} \in \mathbb{R}^{3\times1}$ are representing the rigid transformation from the world to the source coordinates. The calibration matrix $\mathbf{K}_{2D} \in \mathbb{R}^{3\times4}$ defined in the Eq. (1) becomes $\mathbf{K}_{1D} \in \mathbb{R}^{2\times4}$.

$$\mathbf{K}_{1D} = \begin{bmatrix} 0 & \alpha_v & v_0 & 0 \\ 0 & 0 & 1 & 0 \end{bmatrix} \tag{4}$$

The pinhole linear camera model is given by:

$$\begin{bmatrix} sv \\ s \end{bmatrix} = \mathbf{K}_{1D} \begin{bmatrix} \mathbf{R} & \mathbf{t} \\ \mathbf{0}^T & 1 \end{bmatrix} \begin{bmatrix} X \\ Y \\ Z \\ 1 \end{bmatrix} \tag{5}$$

Within the plane Π, *i.e.* using Eq. (3), we can rewrite the Eq. (5) such that the calibration problem is reduced to the estimation of five real parameters n_1, n_2, n_3, n_4, n_5 from :

$$(n_1 - n_4 v)Y + (n_2 - n_5 v)Z + n_3 - v = 0 \tag{6}$$

and the three parameters p, q, r from Eq. (3).

Calibration object The calibration object is made of four co-planar lines. Three of them are parallel and the last one is oblique. For example, we can define these lines within the plane $Z = 0$ by the following equations.

$$\begin{aligned} &(L_1) \quad Y = 0 \\ &(L_2) \quad Y = \xi_1 \\ &(L_3) \quad Y = \xi_2 \\ &(L_4) \quad Y = \alpha X + \beta \end{aligned} \tag{7}$$

The intersections of these lines with the plane Π and their projections on D are used to solve the calibration problem. A key idea introduced by Horaud *et al.* is to use the intersections of (L_1), (L_2) and (L_3) with the plane Π and their projections on D to estimate the intersection point of (L_4) and Π using a projective invariant : the cross-ratio.[1] Therefore, by translating this object several times along the $\mathbf{y}$ and/or $\mathbf{z}$ axes, we can acquire enough data to solve the calibration problem.

Calibration problem We denote $\{Y_i^p, Z_i^p, v_i^p\}$ and $\left\{X_j^o, Y_j^o, Z_j^o\right\}$ the sets of known data related to the parallel and oblique lines, respectively, with $i = 1, \ldots, n_{\mathrm{P}}$ and $j = 1, \ldots, n_{\mathrm{O}}$, where $n_{\mathrm{P}} \geq 5$ and $n_{\mathrm{O}} \geq 3$ are the numbers of parallel and oblique lines, respectively. In Fig. 2 we show a calibration object containing the minimal number of eight calibration lines. Using (6) and the parallels lines set of data, we can estimate the parameters n_1, n_2, n_3, n_4, n_5 by solving a system of n_{P} equations in the least square sense. Likewise, we estimate the viewing plane parameters p, q, r by solving a system of n_{O} equations based on the Eq. (3).

Calibration parameters estimation The intrinsic and extrinsic parameters can easily be extracted from n_1, n_2, n_3, n_4 and n_5 using p, q and r (see[6]). Then, the source position (X_S, Y_S, Z_S) can be estimated by solving the linear system (8) where v^* and $v^\diamond$ are two different detector pixels. Indeed, the source belongs to all the backprojection lines and the viewing plane Π.

$$\begin{cases} (n_1 - n_4 v^*)Y_S + (n_2 - n_5 v^*)Z_S + n_3 - v^* = 0 \\ (n_1 - n_4 v^\diamond)Y_S + (n_2 - n_5 v^\diamond)Z_S + n_3 - v^\diamond = 0 \\ -X_S + pY_S + qZ_S + r = 0 \end{cases} \tag{8}$$

2.3 Multi-detector calibration

The first obvious idea to calibrate a multiple linear detector system would be to use the previous method on each detector. However, all subsystems share the same source. In this section, we present four different methods exploiting this property.
In the following, as in section 2.1, the index l refers to the detector D_l, $l = 1, \dots, n_{\mathrm{D}}$.

Method 1 (M1) We use the previous method on each subsystem to calibrate the system. We then agregate the equations (8) associated to each detector $D_l, l = 1, \dots, n_{\mathrm{D}}$ for estimating an unique source position. The agregated system of equations (9) is composed of $3n_{\mathrm{D}}$ equations and can be easily solved by least squares.

$$\begin{cases} (n_{l,1} - n_{l,4}v_l^*)Y_S + (n_{l,2} - n_{l,5}v_l^*)Z_S = v_l^* - n_{l,3} \\ (n_{l,1} - n_{l,4}v_l^\diamond)Y_S + (n_{l,2} - n_{l,5}v_l^\diamond)Z_S = v_l^\diamond - n_{l,3} \\ -X_S + p_l Y_S + q_l Z_S = -r_l \end{cases} \tag{9}$$

Method 2 (M2) From the combination of the equations (3) and (9), we get a system of $(n_{\mathrm{O}}+3)n_{\mathrm{D}}$ non-linear equations (10) in the parameters p_l, q_l, r_l, X_S, Y_S and Z_S, $l = 1, \dots, n_{\mathrm{D}}$.

$$\begin{cases} (n_{l,1} - n_{l,4}v_l^*)Y_S + (n_{l,2} - n_{l,5}v_l^*)Z_S = v_l^* - n_{l,3} \\ (n_{l,1} - n_{l,4}v_l^\diamond)Y_S + (n_{l,2} - n_{l,5}v_l^\diamond)Z_S = v_l^\diamond - n_{l,3} \\ -X_S + p_l Y_S + q_l Z_S + r_l = 0 \\ p_l Y_{l,j}^o + q_l Z_{l,j}^o + r_l = X_{l,j}^o, \quad j = 1, \dots, n_{\mathrm{O}} \end{cases} \tag{10}$$

This system can be solved using the Gauss-Newton algorithm. We suggest to initialize the algorithm with the results of M1.

Method 3 (M3) Similarly to M2, by combining the equations (6) and (9), we build a system of $(n_{\mathrm{P}}+3)n_{\mathrm{D}}$ non-linear equations (11) in the parameters $n_{l,1}$, $n_{l,2}$, $n_{l,3}$, $n_{l,4}$, $n_{l,5}$, X_S, Y_S and Z_S, $l = 1, \dots, n_{\mathrm{D}}$.

$$\begin{cases} (n_{l,1} - n_{l,4}v_l^*)Y_S + (n_{l,2} - n_{l,5}v_l^*)Z_S + n_{l,3} = v_l^* \\ (n_{l,1} - n_{l,4}v_l^\diamond)Y_S + (n_{l,2} - n_{l,5}v_l^\diamond)Z_S + n_{l,3} = v_l^\diamond \\ -X_S + p_l Y_S + q_l Z_S = -r_l \\ (n_{l,1} - n_{l,4}v_{l,i}^p)Y_{l,i}^p + (n_{l,2} - n_{l,5}v_{l,i}^p)Z_{l,i}^p + n_{l,3} = v_{l,i}^p, \\ \qquad\qquad i = 1, \dots, n_{\mathrm{P}} \end{cases} \tag{11}$$

We use the same numerical method as for M2 for solving Eq. (11).

Method 4 (M4) The last method combines the equations of M2 and M3. Consequently, the system of $(n_{\mathrm{P}}+n_{\mathrm{O}}+3)n_{\mathrm{D}}$ equations (12) to solve is non-linear in the parameters p_l, q_l, r_l, $n_{l,1}$, $n_{l,2}$, $n_{l,3}$, $n_{l,4}$, $n_{l,5}$, X_S, Y_S and Z_S, $l = 1, \dots, n_{\mathrm{D}}$.

$$\begin{cases} (n_{l,1} - n_{l,4}v_l^*)Y_S + (n_{l,2} - n_{l,5}v_l^*)Z_S + n_{l,3} = v_l^* \\ (n_{l,1} - n_{l,4}v_l^\diamond)Y_S + (n_{l,2} - n_{l,5}v_l^\diamond)Z_S + n_{l,3} = v_l^\diamond \\ -X_S + p_l Y_S + q_l Z_S + r_l = 0 \\ p_l Y_{l,j}^o + q_l Z_{l,j}^o + r_l = X_{l,j}^o, \quad j = 1, \dots, n_{\mathrm{O}} \\ (n_{l,1} - n_{l,4}v_{l,i}^p)Y_{l,i}^p + (n_{l,2} - n_{l,5}v_{l,i}^p)Z_{l,i}^p + n_{l,3} = v_{l,i}^p, \\ \qquad\qquad i = 1, \dots, n_{\mathrm{P}} \end{cases} \tag{12}$$

The resolution can be done using the Gauss-Newton algorithm as for M2 and M3.

2.4 Calibration object

The use of sufficient four co-planar lines calibration objects presented in the section 2.2 could be enough to generate the data required to solve the calibration problem. Nevertheless, we present in this section several improvements.

Minimal calibration object The first improvement is to construct a minimal calibration object composed of 5 parallel lines and 3 oblique lines. The parallel lines are shared among the oblique lines such that 3 groups of 3 parallel plus one oblique line, as in section 2.2, can be provided. The 5 parallel lines are defined by the equations (13).

$$\begin{aligned}
&(L_1) \quad Z = 0, \quad && Y = 0 \\
&(L_2) \quad Z = 0, \quad && Y = \varepsilon \\
&(L_3) \quad Z = 0, \quad && Y = 2\varepsilon \\
&(L_4) \quad Z = -\eta, \quad && Y = 2\varepsilon \\
&(L_5) \quad Z = -2\eta, \quad && Y = 2\varepsilon
\end{aligned} \tag{13}$$

The three oblique lines are defined by the equations (14).

$$\begin{aligned}
&(L_6) \quad Z = 0, \quad && Y = \frac{\varepsilon}{2W}X + \frac{\varepsilon}{2} \\
&(L_7) \quad Z = 0, \quad && Y = \frac{\varepsilon}{2W}X + \frac{5\varepsilon}{2} \\
&(L_8) \quad Y = 2\varepsilon, \quad && Z = -\frac{\eta}{2W}X - \frac{\eta}{2}
\end{aligned} \tag{14}$$

The minimal calibration object is illustrated in the Fig. 2. One can notice that the group of lines in the plane $Y = 2\varepsilon$ doesn't result from a translation as suggested in the section 2.2. The cross-ratio can be adapted in this plane. Besides, we remark that the lines are positioned such that their projections can be spanned all over the detectors using an adequate value of ε.

Adapted object First, we observed that adding to the minimal calibration object the parallel line (L_9) defined in the Eq. (15) improved significantly the accuracy of the calibration.

$$(L_9) \quad Z = 0, \quad Y = 3\varepsilon \tag{15}$$

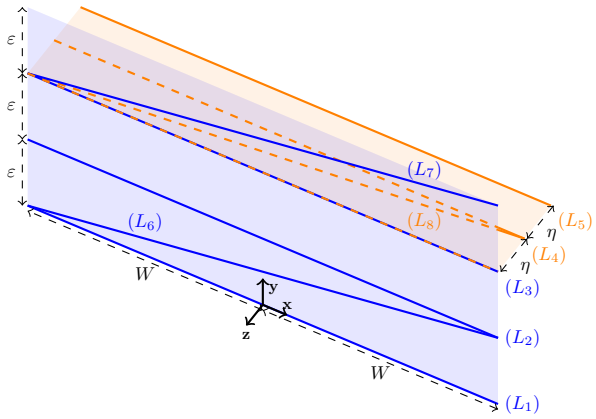

Figure 2: The minimal calibration object.

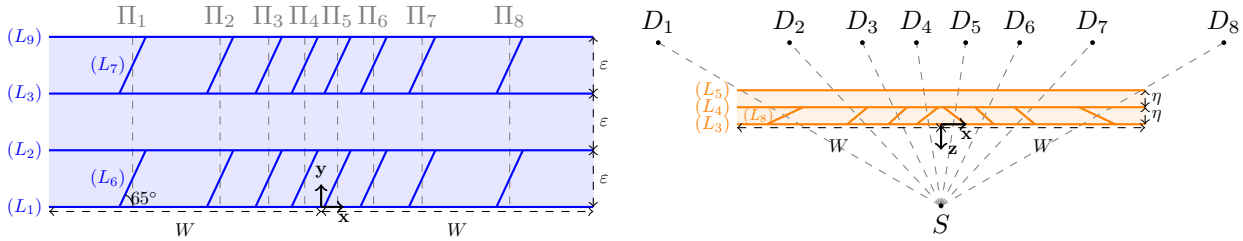

(a) (b)

Figure 3: (a) Vertical plane and (b) horizontal plane of the object used for the 8-detectors system calibration.

Then, another improvement is the positioning of the oblique lines relatively to each detector D_l, $l = 1, \ldots, n_{\mathrm{D}}$. The lines are placed such that the intersections of the oblique lines and the viewing planes are at equal distance of the two closest co-planar parallel lines. We denote these lines $(L_{6,l})$, $(L_{7,l})$ and $(L_{8,l})$, $l = 1, \ldots, n_{\mathrm{D}}$. The lines $(L_{6,l})$ and $(L_{7,l})$ are positioned in the plane $Z = 0$ between the lines (L_1) and (L_2), and the lines (L_3) and (L_9), respectively. They are inclined at a fixed angle λ. The lines $(L_{8,l})$ are positioned in the plane $Y = 2\varepsilon$, between the lines (L_3) and (L_4). The inclinations of these lines are specific to each detector. Nevertheless, the position of the lines $(L_{8,l})$ doesn't impact the results as much as the two others obliques lines. Thus, every way of positioning the lines can be used providing that the intersection of the lines and the viewing planes are at $Z = -\frac{\eta}{2}$. An example of such a calibration object is given in the Fig. 3.

3. SIMULATION

We consider a 8-linear-detector system. The distance from the source to the plane containing the detectors is $480mm$. The detectors are spaced at a constant angle from the source. The calibration object is positioned halfway between the source and the detectors line. The detectors have 1920 pixels of height $0.4mm$. The parameters of the calibration object are set to $W = 600mm$, $\varepsilon = 125mm$ and $\eta = 50mm$. The two planes containing line segments of the calibration object are illustrated in the Fig. 3a and 3b, respectively.

We begin with the comparison of the methods presented in the section 2.3. The methods are compared on the average projection errors observed on 100 simulations where we add Gaussian noise $\mathcal{N}(0, \sigma^2)$ to the data. The value of σ is set as a fraction of the pixels size.

The average projection errors are calculated by computing the absolute value of the difference between the theoretical projections of 2 oblique lines and the projections obtained using successively the Eq. (3) to compute

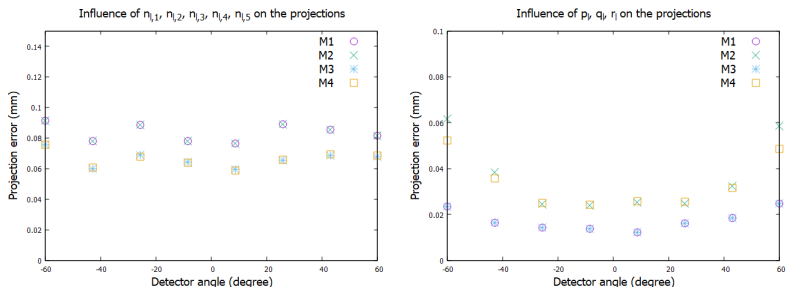

(a) (b)

Figure 4: Methods comparison. The graphics show the average projection errors of 2 oblique lines on the 8 detectors using the estimated values of (a) the parameters $n_{l,1}$, $n_{l,2}$, $n_{l,3}$, $n_{l,4}$, $n_{l,5}$ (b) the parameters p_l, q_l, r_l, with $\sigma = 0.24px$, $l = 1, \ldots, n_{\mathrm{D}}$.

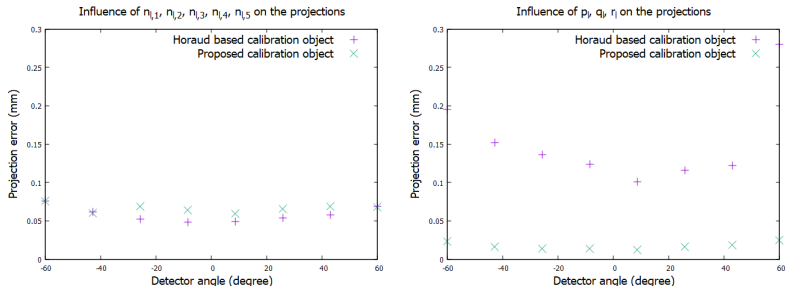

(a) (b)

Figure 5: Calibration objects comparison. The graphics show the average projection errors of 2 oblique lines on the 8 detectors using the estimated values of (a) the parameters $n_{l,1}$, $n_{l,2}$, $n_{l,3}$, $n_{l,4}$, $n_{l,5}$ (b) the parameters p_l, q_l, r_l, with $\sigma = 0.24px$, $l = 1, \ldots, n_{\mathrm{D}}$.

the intersections of the oblique lines and Π_l, and the Eq. (6) to compute the projections of the intersections points. Two projections are calculated using the estimated values of either the parameters $n_{l,1}$, $n_{l,2}$, $n_{l,3}$, $n_{l,4}$, $n_{l,5}$ or the parameters p_l, q_l, r_l. The results are presented in the Fig. 4.

It can be observed in the Fig. 4a that M3 and M4 improve slightly the estimation of the parameters $n_{l,1}$, $n_{l,2}$, $n_{l,3}$, $n_{l,4}$, $n_{l,5}$. We can see in the Fig. 4b that M2 and M4 fail to improve the estimation of the viewing planes parameters whereas M1 and M3 have the lowest errors.
Finally, we compare the results of the proposed calibration object with those obtained with the object presented in the section 2.2. We consider here only one wide object for all the detectors. We set $\xi_1 = \xi_2 = 100mm$, $\alpha = 0.25$ and $\beta = 75$. The object is initially positioned in-between the source and the detectors line. Then, it is shifted twice on the $\mathbf{y}$ and $\mathbf{z}$ axes. Exactly, we shift the object successively by $Y_{shift} = 200mm$ along the $\mathbf{y}$ axis and by $Z_{shift} = -150mm$ along the $\mathbf{z}$ axis. We use M3 to solve the problem. The results are presented in the Fig. 5. We can see in the Fig. 5a that the objects achieves comparable results on the estimation of the parameters $n_{l,1}$, $n_{l,2}$, $n_{l,3}$, $n_{l,4}$ and $n_{l,5}$. However, we can observe in the Fig. 5b that the estimation of the viewing planes parameters are much better with the calibration object proposed in 2.4.

4. CONCLUSION

We have extended the linear camera geometric calibration method introduced by Horaud *et al.*[6] (see section 2.2) to a multiple linear detector system. We have proposed a minimal calibration phantom of 8 opaque lines. But we have observed that adding one opaque line improves highly the accuracy and the stability of the calibration parameter estimation. This calibration object has been adapted to a multiple linear detector system in order to preserve a sufficient oblicity for the oblique lines. We have proposed and evaluated 4 numerical methods exploiting the fact that all subsystems share the same x-ray source.
Our numerical simulations have shown that estimating the geometric parameters of multi linear detector systems taking into account that they share the same x-ray source, improves the geometric calibration.

REFERENCES

1. R. Hartley and A. Zisserman, *Multiple View Geometry in Computer Vision*, Cambridge University Press, second ed., 2004.
2. R. Tsai, "A versatile camera calibration technique for high-accuray 3d machine vision metrology off-the-shelf tv cameras and lenses," *IEEE Journal of Robotics and Automation* **RA-3**(4), pp. 323–344, 1987.
3. F. Noo, R. Clackdoyle, C. Mennessier, T. White, and T. Roney, "Analytic method based on identification of ellipse parameters for scanner calibration in cone-beam tomography," *Physics in Medicine and Biology* **45**(11), pp. 3489–3508, 2000.
4. Y. Cho, D. Moseley, J. Siewerdsen, and D. Jaffray, "Accurate technique for complete geometric calibration of cone-beam computed tomography systems," *Medical Physics* **32**(4), pp. 968–983, 2005.
5. M. J. Daly, J. H. Siewerdsen, Y. B. Cho, D. A. Jaffray, and J. C. Irish, "Geometric calibration of a mobile c-arm for intraoperative cone-beam ct," *Medical Physics* **35**(5), pp. 2124–2136, 2008.
6. R. Horaud, R. Mohr, and B. Lorecki, "On single-scanline camera calibration," *IEEE Transactions on Robotics and Automation* **1**(9), pp. 71–75, 1993.